Scientific Research Publishing

Open Journal of Metal, 2021, 11, 11-20
https://www.scirp.org/journal/ojmetal
ISSN Online: 2164-277X
ISSN Print: 2164-2761

Influence of Plastic Deformation and Aging Process on Microstructure and Tensile Properties of Cast Ti-6Al-2Sn-2Zr-2Mo-1.5Cr-2Nb-0.1Si Alloy

Mostafa S. S. El-Deeb[1], Khaled M. Ibrahim[2], S. S. Mohamed[3], Ramadan N. Elshaer[4*]

[1]Modern Academy for Engineering and Technology, Cairo, Egypt
[2]Central Metallurgical R & D Institute, Cairo, Egypt
[3]Shoubra Faculty of Engineering, Benha University, Cairo, Egypt
[4]Tabbin Institute for Metallurgical Studies, Cairo, Egypt
Email: *ramadan_elshaer@yahoo.com

How to cite this paper: El-Deeb, M.S.S., Ibrahim, K.M., Mohamed, S.S. and Elshaer, R.N. (2021) Influence of Plastic Deformation and Aging Process on Microstructure and Tensile Properties of Cast Ti-6Al-2Sn-2Zr-2Mo-1.5Cr-2Nb-0.1Si Alloy. *Open Journal of Metal*, **11**, 11-20.
https://doi.org/10.4236/ojmetal.2021.112002

Received: March 2, 2021
Accepted: June 14, 2021
Published: June 17, 2021

Abstract

In the present work, titanium alloy with a composition of Ti-6.5Al-3Mo-1.9Nb-2.2Sn-2.2Zr-1.5Cr (TC21) was subjected to plastic deformation and aging processes. A Plastic deformation at room temperature with 2%, 3% and 4% stroke strain was applied on the studied samples. Then, the samples aged at 575˚C for 4 hr. By applying different plastic deformation ratios, the structure revealed an elongated and thin β-phase embedded in an α-phase. Secondary α-platelets were precipitated in the residual β-phase. Maximum hardness (HV440) was obtained for 4% deformed + aged samples. Minimum hardness (HV320) was recorded for the as-cast samples without deformation. The highest ultimate tensile strength of 1311 MPa was obtained for 4% deformed + aged samples due to presence of high amount of dislocation density as well as precipitation of secondary α-platelets in the residual β-phase. The lowest ultimate tensile strength of 1020 MPa was reported for as-cast samples. Maximum elongation of 14% was registered for 4% deformed + aged samples and minimum one of 3% was obtained for as-cast samples. Hence, strain hardening + aging can enhance considerably the elongation of TC21 Ti-alloy up to 366% and 133% in case of applying 4% deformation + aged compared to as-cast and aged samples without applying plastic deformation, respectively.

Keywords

TC21 Ti-Alloy, Strain Hardening, Microstructure, Aging, Hardness, Tensile

1. Introduction

Titanium alloys, especially $\alpha + \beta$, exhibited a combination of high strength-to-weight ratio, good fatigue performance, excellent corrosion resistance that make them the best material choice for some critical applications such as advanced aerospace applications, petroleum sector and chemical industries [1] [2] [3] [4]. Titanium and its alloys are heat-treated for many reasons, such as 1) reduce residual stresses developed during fabrication/casting process (stress relieving), 2) produce an optimum combination of ductility, machinability, and structural stability (annealing), 3) increase strength and fatigue performance (solution treating and aging). Strain hardening phenomenon of titanium alloys has been extensively studied since the evolution of dislocation theory and is still being investigated and correlated. Basically, it results from the interaction of dislocation with each other and with the various constituents of the microstructure such as grain boundaries, precipitates and solutes, etc. TC21 Ti-alloy is a new α/β high strength and toughness alloy as a candidate material for structural parts of advanced aircraft [5] [6] [7] [8]. TC21 Ti-alloy has increased room-temperature strength and better damage tolerance properties compared to Ti6Al4V [9] [10]. TC21 Ti-alloy exhibits also excellent superplasticity that provides guidance to develop superplastic-forming technology. Titanium alloys have become one of the indispensable structure materials for airplanes. They are used in advanced airplanes up to 30% - 50% weight of the total structure such as landing gear and flap track [11]. After applying deformation (strain hardening) and heat treatment at a certain temperature, microstructures of TC21 Ti-alloy will be changed for getting better mechanical properties. Microstructure parameters including volume fraction, grain size, geometric morphology and distribution of the existing two phases ($\alpha + \beta$) significantly affect the performance of titanium alloys [7] [8]. Many studies focus on the effects of plastic deformation and heat treatment process on microstructure and mechanical properties of TC21 Ti-alloy [12] [13] [14] [15] [16]. Y. Fei *et al.* [17] studied phase transformation and microstructure of TC21 alloy under different heat-treatment. The result showed that heat-treatment parameters (solution temperature and cooling rate) had an influence on the feature of α, β and secondary α phases. H. Shao *et al.* [18] investigated the effect of tensile deformation process on lamellar microstructure in TC21 Ti-alloy by scanning electron microscopy (SEM). The results showed that slip band primarily appeared in stress concentration region and then broadened. Micro-cracks mainly initiated on the interface of α lamellae at the side of sample and subsequently propagated. The path of crack propagation was related to the included angle between α colony and tensile direction. R.K. Gupta *et al.* [19] studied strain hardening of titanium alloy Ti6Al4V sheets with prior heat treatment and cold working. The result showed that strain hardening exponent (n) is found to be decreased with increasing strain rates for the samples at all heat treatment conditions. The present work aims at studying the effect of strain hardening and aging process on microstructure and tensile properties of cast

TC21 Ti-alloy.

2. Materials and Experimental Procedures

2.1. Material

TC21 Ti-alloy samples were cast as ingots using a vacuum induction skull melting (ISM) furnace in a graphite mould. Before melting, the graphite mould was preheated in the heating chamber inside the ISM furnace to 900˚C. Hereafter, the raw TC21 Ti-material is heated to reach 1700˚C to melt it under vacuum that reached to 4×10^{-2} mbar. The samples cast in a graphite mould as 30 mm in diameter and 300 mm long. Then, they were machined to reduce the bar size into 25 mm diameter and 250 mm long. Hot swaging process was applied at 700˚C to reduce the diameter to 8 mm at 12 steps. Annealing process was applied at 550˚C for 2 hr followed by furnace cooling to reduce residual stress resulting from swaging process. The chemical composition of the investigated TC21 Ti-alloy is given in Table 1.

2.2. Experimental Procedures

The samples were classified into four groups, where the first group was as-cast samples, the second group was swaged + annealed samples, and the third group was aged samples at 575˚C/4hr after swaging and annealing processes. Plastic deformation (strain hardening) process was applied at room temperature with 2%, 3% and 4% strain fourth group using a universal tensile testing machine Hereafter, aging treatment was applied at 575˚C at 4 hr. The samples were prepared for metallography work by grinding, polishing and etching using a solution consisting of 3% HF, 30% HNO_3 and 67% H_2O. The samples were metallography examined using field emission scanning electron microscope (FESEM). Vickers hardness was carried out in accordance to ASTM E92-16 Standard. The samples were machined to 4 mm diameter with a gage length of 20 mm to determine the tensile properties. Tensile testing was carried out according to ASTM E8/E8M-16 Standard at room temperature using a strain rate of 1 mm/min. Fractography of some selected fracture tensile samples was analyzed and examined using FESEM.

3. Results and Discussion

3.1. Microstructure Evolution

Microstructure of as-cast TC21 Ti-alloy showed a matrix consisting of equiaxed β-phase and various morphologies of α-phase. The α-phase was located between the β-phase in the matrix and also at the grain boundaries. The average β-grain

Table 1. Chemical composition of TC21 Ti-alloy (mass fraction, %).

Al	Mo	Nb	Sn	Zr	Cr	Si	Fe	C	N	H	O	Ti
6.10	2.96	2.11	1.98	2.05	1.44	0.10	0.07	0.01	0.02	0.003	0.10	Bal

size was in the range of 150 - 250 μm as shown in **Figure 1(a)**. These results are in good agreement with previous works done by M. J. Bermingham *et al.* [20] and I. N. Jujur *et al.* [21]. These coarse grains are normally specified to the cast Ti-structure. The feature of α & β phases in the grains can be specified as lamellar structure. By applying swaging process on the as-cast samples, the structure obtained fine structure consisting of primary equiaxed α phase (α_p), (dark color), and transformed β-phase (β_{trans}), (gray color), **Figure 1(b)**. The average grain size of α-phase was in the range of 2.3 μm and its volume fraction approached 63% using image analyzer. The equiaxed α-phase was distributed homogeneously in the entire field of view. The XRD pattern confirmed the presence of α and β phases in the as-cast structure, **Figure 2**. In **Figure 1(c)**, FESEM of the aged samples at 575˚C/4hr showed equiaxed structure that composed of primary α-phase (α_p) distributed homogenously in a transformed β-phase (β_{trans}). In addition, secondary α-phase (α_s) was nucleated at the transformed β-phase as a result of aging process. Volume fractions of α_p, β_{trans} and α_s were in the ranges of

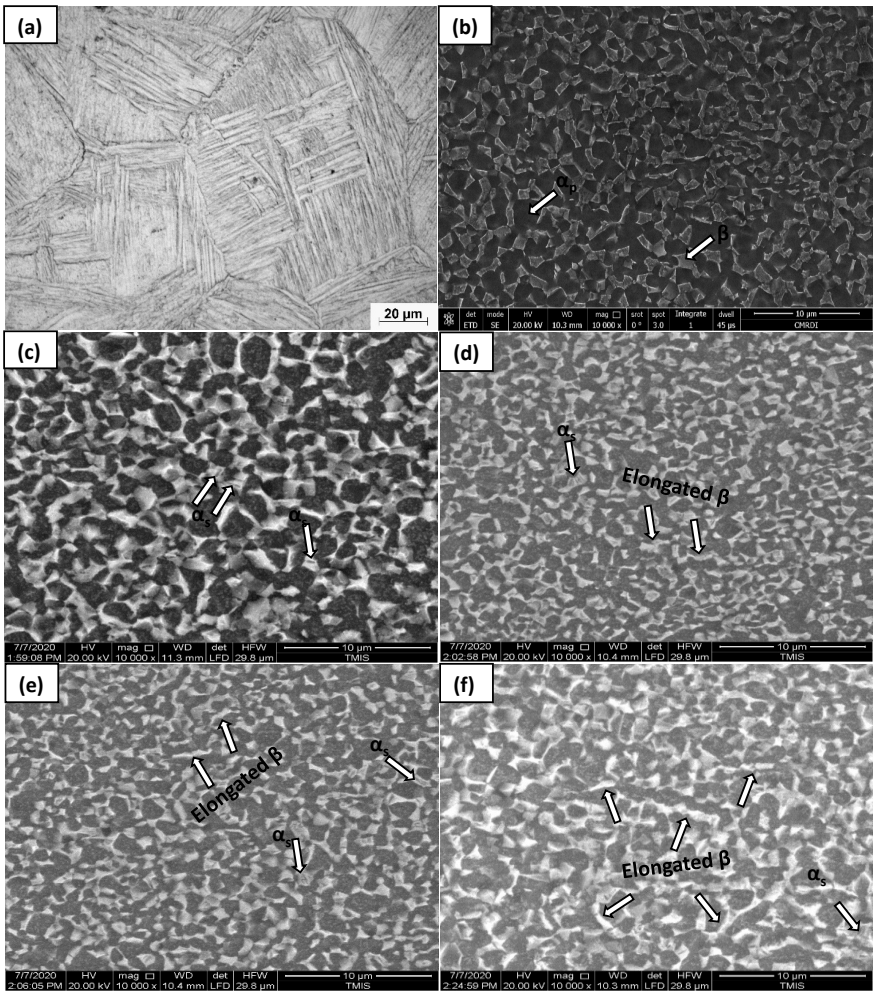

Figure 1. FESEM micrographs showing the microstructures of conditions (a) as-cast, (b) swaged, (c) aging only, (d) 2% Def + aging, (e) 3% Def + aging and (f) 4% Def + aging, samples of TC21Ti-alloy.

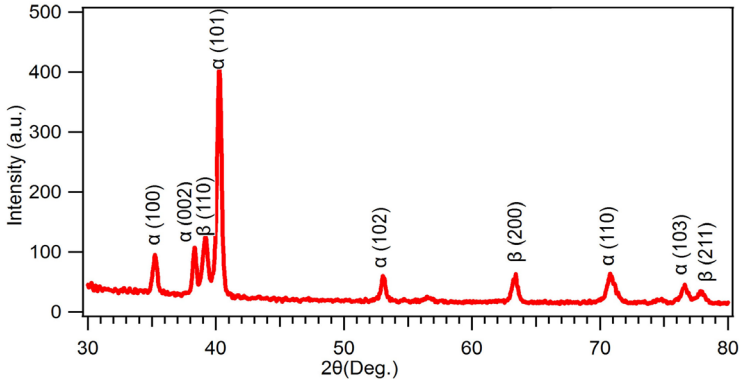

Figure 2. XRD pattern of the as-cast TC21 Ti-alloy.

63%, 31% and 6%, respectively. These fine α_s were precipitated from the supersaturated β-phase during aging process. The precipitated α_s platelets on β-phase have a big role in increasing the strength of the studied TC21 alloy. The last group of the samples was subjected to plastic deformation by tension + aging at 575˚C/4hr. The microstructure of this group showed also equiaxed structure that composed of α_p, α_s and β_{trans} phases, **Figures 1(d)-(f)**. This structure is similar to the aged samples, but the difference was located in the β-phase. The transformed β-phase after applying plastic deformation obtained an elongated shape that depends on the percentage of the plastic deformation (2%, 3% &4%). The percentage of elongation of transformed β-phase increases with increasing the percentage of deformation 2% to 4%. By elongating the transformed β-phase, the matrix can be described as isolated islands of β-phase in α-matrix as comparing to the swaged or aged samples. The XRD pattern confirmed the presence of α_p, α_s and β_t phases in the aging only and 4% Def + aging conditions, **Figure 3**.

3.2. Hardness Test

Vickers hardness was carried out to evaluate the hardness of as-cast, swaged, aged samples and also to investigate the influence of strain hardening on TC21 Ti-alloy, **Figure 4**. As-cast samples revealed the lowest hardness (HV320) due to existence of coarse structure as well as presence of heterogeneity in the $\alpha + \beta$ structure. While, the swaged samples obtained a higher hardness of (HV353) compared to the as-cast samples owing to the refined structure that caused by applying severe plastic deformation via swaging process. Samples with 2% strain hardening showed a relative high hardness (HV398). The deformed samples at strain rate of 4% obtained the highest hardness value of (HV440) due to the following reasons: 1) The presence of high amount of dislocation density caused by of high percentage of strain hardening (plastic deformation). 2) Existing of α_s-platelets that were precipitated in the β_{trans} phase and 3) Increasing the percentage of elongated β phase with increasing the percentage of deformation from 2% to 4%. Hence, the hardness increased in the structure. Comparing to the aged samples, there was an increase in hardness of deformed samples with 4% + aging reached to 36%. But this increase in hardness reached to 38% by comparing

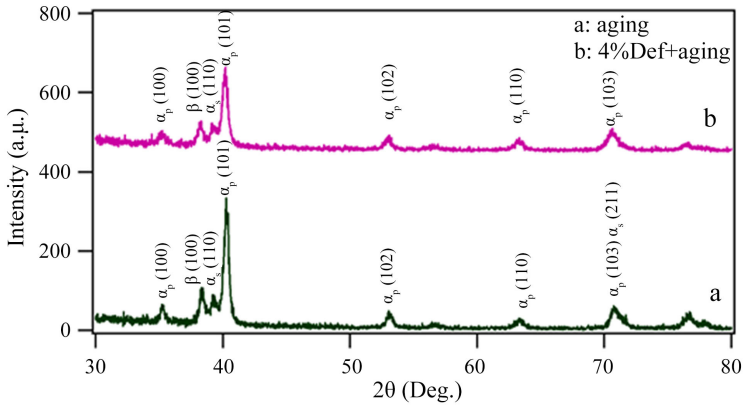

Figure 3. XRD pattern of aging only and 4% Def + aging conditions.

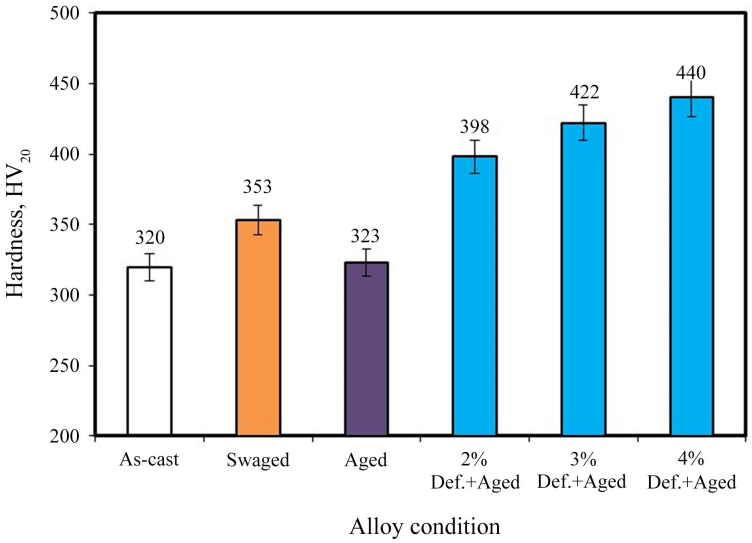

Figure 4. Average hardness values at various conditions.

to the as-cast samples. Therefore, it can be concluded here that 4% deformation + aging samples showed the highest hardness compared to the other conditions.

3.3. Tensile Properties

The tensile properties of TC21 Ti-alloy for as-cast, swaged, aged, and deformed + aging samples are shown in Figure 5. Both yield and ultimate tensile strengths increased after applying aging compared to as-cast and swaged samples. This is due to forming of α_s due to aging process. There was also relative increase in both yield and ultimate strengths after applying plastic deformation. Maximum ultimate strength (1311 MPa) was reported for the samples plastically deformed at 4% deformed + aging. The same behavior was shown for yield strength, where maximum yield strength was 1233 MPa. This is due to the presence of high amount of dislocation density as well as precipitation of secondary α-platelets in β_{trans} phase. While the lowest yield and ultimate strengths of 900 MPa and 1020 MPa were reported for the as-cast samples. This is due to the heterogeneity ex-

isting in the structure as well as the large scale of grain boundaries. Figure 6 showed the percentage of elongation for the investigated samples. Maximum elongation of 14% was reported for 4% deformed + aging samples and minimum one of 3% was obtained for as-cast samples. Maximum elongation of deformed + aged samples was due to the nature of microstructure which is composed of α-matrix and discontinuity transformed β-phase imbedded in the α-matrix. Because of the discontinuity of β-phase after applying deformation, there was a chance for stretching the α-phase during the tensile deformation. Hence, the elongation will be highly dependent on the α-phase. Therefore, the samples deformed at 4% + aging gave the highest elongation percentage of 14%. However, the as-cast structure gave the lowest elongation of 3% due to heterogeneity in structure as well as the coarse grain size. As a conclusion, the elongation can be reached to the highest value by applying a plastic deformation at 4% and followed by aging process at 575˚C/4hr.

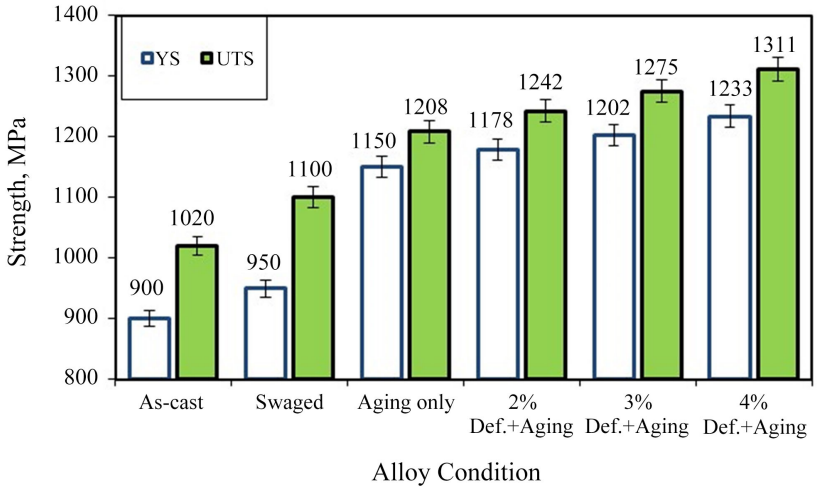

Figure 5. Variation of YS and UTS at various conditions.

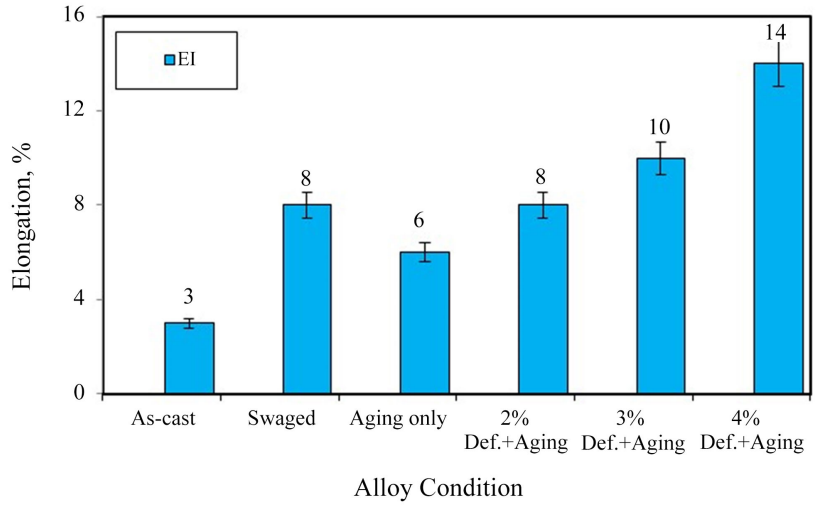

Figure 6. Variation of elongation at various conditions.

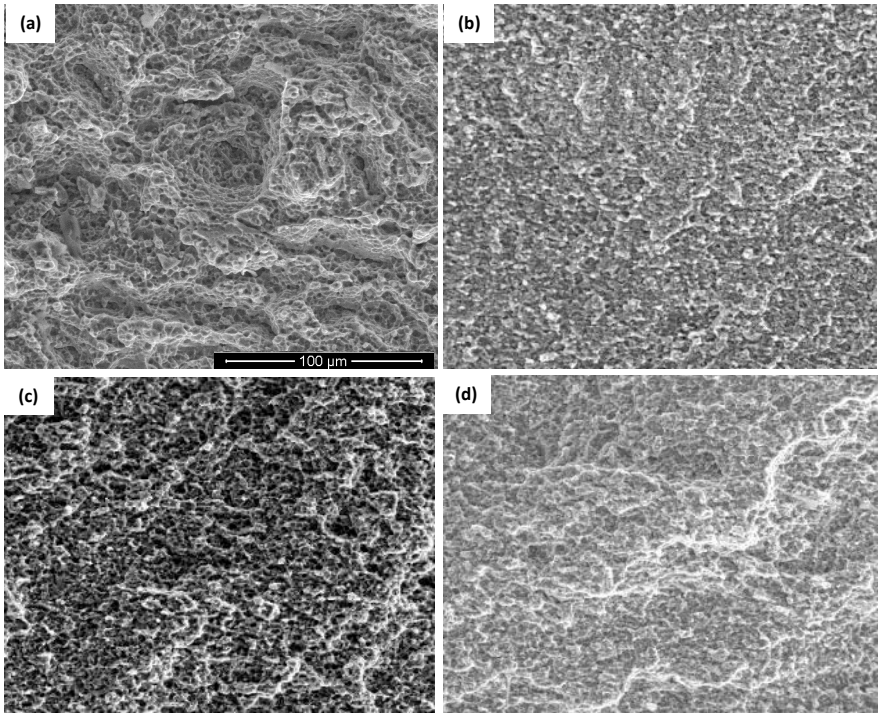

Figure 7. Fracture surface of tensile samples (a) swaged, (b) aging only, (c) 2% Def + aging and (d) 4% Def + aging.

Tensile Fractography

The fracture surface of some selected tensile samples (swaged, aged, 2% Def + aging, and 4% Def + aging) was examined using FESEM, **Figure 7**. Swaged samples showed high amount of dimples which indicated the high ductility of the sample. However, aged samples revealed a brittle fracture feature with low amount of dimples. The dimples existing in the fracture surface is referring to α-phase in the structure. The deformed samples at (2% Def + aging) showed the same feature of the aged samples, but with higher amount of dimples. These dimples revealed existing of relative high amount of α-phase compared to the last one. Maximum amount of dimples were noticed in the fracture surface of the samples that was deformed at 4%. The nature of the microstructure plays an important role in determining the fracture feature. Because of existing discontinuity in β-phase, there was a big chance for occurring a ductile fracture (dimples) due to existing high amount of α-phase in matrix.

4. Conclusions

1) As-cast microstructure showed a matrix consisting of β-grains and various morphologies of α-phase. The average β-grain size was in the range of 150 - 250 µm.

2) Microstructure of swaged samples consisted of primary equiaxed α phase and transformed β phase. The average grain size of α phase was in the range of 2.3 µm and its volume fraction approached 63%.

3) Mechanical properties increased with increasing the percentage of defor-

mation from 2% to 3% to 4% deformation.

4) Optimum ultimate tensile strength of 1311 MPa was obtained for 4% deformed + aged samples due to presence of high amount of dislocation density as well as precipitation of secondary α-platelets in the residual β-phase.

5) The lowest ultimate tensile strength of 1020 MPa was reported for as-cast samples.

6) Maximum elongation of 14% was observed for 4% deformed + aged samples and minimum one of 3% was obtained for as-cast samples.

Conflicts of Interest

The authors declare no conflicts of interest regarding the publication of this paper.

References

[1] Ibrahim, K.M., EL-Hakeem, A.M.M. and Elshaer, R.N. (2013) Microstructure and Mechanical Properties of Cast and Heat Treated Ti-6.55Al-3.41Mo-1.77Zr Alloy. *Transactions of Nonferrous Metals Society of China*, **23**, 3517-3524. https://doi.org/10.1016/S1003-6326(13)62896-4

[2] Elshaer, R.N., Ibrahim, K.M., Lotfy, I. and Abdel-Latif, M.A. (2020) Effect of Cooling Rate and Aging Process on Wear Behavior of TC21 Ti-Alloy. *Key Engineering Materials*, **835**, 265-273. https://doi.org/10.4028/www.scientific.net/KEM.835.265

[3] Wang, L., Zang, Q.Y., Li, X.X., Cui, X.H. and Wang, S.Q. (2014) Severe-to-Mild Wear Transition of Titanium Alloys as a Function of Temperature. *Tribology Letters*, **53**, 511-520. https://doi.org/10.1007/s11249-013-0289-5

[4] Zhang, Q.Y., Zhou, Y., Li, X.X., Wang, L., Cui, X.H. and Wang, S.Q. (2016) Accelerated Formation of Tribo-Oxide Layer and Its Effect on Sliding Wear of a Titanium Alloy. *Tribology Letters*, **63**, Article No. 2. https://doi.org/10.1007/s11249-016-0694-7

[5] Kuruvila, M., Srivatsan, T.S., Petraroli, M. and Park, L. (2008) An Investigation of Microstructure, Hardness, Tensile Behaviour of a Titanium Alloy: Role Orientation. *Sadhana*, **33**, 235-250. https://doi.org/10.1007/s12046-008-0017-2

[6] Wang, X.-L., Zhao, Y.-Q., Wei, X.-W. and Hou, H.-L. (2014) Microstructures of TC21 Alloys after Hydrogenation and Dehydrogenation. *Transactions of Nonferrous Metals Society of China*, **24**, 82-88. https://doi.org/10.1016/S1003-6326(14)63031-4

[7] Wang, Y., Kou, H., Chang, H., Zhu, Z., Su, X., Li, J. and Zhou, L. (2009) Phase Transformation in TC21 Alloy during Continuous Heating. *Journal of Alloys and Compounds*, **472**, 252-256. https://doi.org/10.1016/j.jallcom.2008.04.035

[8] Shao, H., Zhao, Y., Ge, P. and Zeng, W. (2013) Materials Science & Engineering A Crack Initiation and Mechanical Properties of TC21 Titanium Alloy with Equiaxed Microstructure. *Materials Science and Engineering*: *A*, **586**, 215-222. https://doi.org/10.1016/j.msea.2013.08.012

[9] Zhang, Q., Chen, J., Tan, H., Lin, X. and Huang, W.D. (2016) Influence of Solution Treatment on Microstructure Evolution of TC21 Titanium Alloy with near Equiaxed β Grains Fabricated by Laser Additive Manufacture. *Journal of Alloys and Compounds*, **666**, 380-386. https://doi.org/10.1016/j.jallcom.2016.01.065

[10] Kikuchi, S., Yoshida, S. and Ueno, A. (2019) Improvement of Fatigue Properties of

Ti-6Al-4V Alloy under Four-Point Bending by Low Temperature Nitriding. *International Journal of Fatigue*, **120**, 134-140. https://doi.org/10.1016/j.ijfatigue.2018.11.005

[11] Guo, L., Fan, X., Yu, G. and Yang, H. (2016) Microstructure Control Techniques in Primary Hot Working of Titanium Alloy Bars: A Review. *Chinese Journal of Aeronautics*, **29**, 30-40. https://doi.org/10.1016/j.cja.2015.07.011

[12] Ling, Z. and Dong, H. (2013) Microstructure of TC21 Titanium Alloy after Superplastic Deformation and Heat Treatment. *Applied Mechanics and Materials*, **277**, 1855-1858. https://doi.org/10.4028/www.scientific.net/AMM.275-277.1855

[13] Zhang, L. and Tian, J. (2009) Effects of Heat Treatment on Microstructures and Mechanical Performances of TC21 Titanium Alloy Forgings. *Materials Science*, **9-10**, 84-87.

[14] Wang, K., Wu, M., Yan, Z., Li, D., Xin, R. and Liu, Q. (2018) Dynamic Restoration and Deformation Heterogeneity during Hot Deformation of a Duplex-Structure TC21 Titanium Alloy. *Materials Science and Engineering*: *A*, **712**, 440-452. https://doi.org/10.1016/j.msea.2017.11.127

[15] Wen, X., Wan, M., Huang, C., Tan, Y., Lei, M., Liang, Y. and Cai, X. (2019) Effect of Microstructural on Tensile Properties, Impact Toughness and Fracture Toughness of TC21 Alloy. *Materials and Design*, **180**, Article ID: 107899. https://doi.org/10.1016/j.matdes.2019.107898

[16] Elshaer, R.N. and Ibrahim, K.M. (2020) Effect of Cold Deformation and Heat Treatment on Microstructure and Mechanical Properties of TC21 Ti Alloy. *Transactions of Nonferrous Metals Society of China*, **30**, 1290-1299. https://doi.org/10.1016/S1003-6326(20)65296-7

[17] Fei, Y., Zhou, L., Qu, H., Zhao, Y. and Huang, C. (2008) The Phase and Microstructure of TC21 Alloy. *Materials Science and Engineering*: *A*, **494**, 166-172. https://doi.org/10.1016/j.msea.2008.04.017

[18] Shao, H., Zhao, Y., Ge, P. and Zeng, W. (2013) In-Situ SEM Observations of Tensile Deformation of the Lamellar Microstructure in TC21 Titanium Alloy. *Materials Science and Engineering*: *A*, **559**, 515-519. https://doi.org/10.1016/j.msea.2012.08.134

[19] Gupta, R.K., Kumar, V.A., Mathew, C. and Rao, G.S. (2016) Strain Hardening of Titanium Alloy Ti6Al4V Sheets with Prior Heat Treatment and Cold Working. *Materials Science and Engineering*: *A*, **662**, 537-550. https://doi.org/10.1016/j.msea.2016.03.094

[20] Bermingham, M., Mcdonald, S.D., Dargusch, M.S. and Stjohn, D.H. (2007) Microstucture of Cast Titanium Alloys. *Materials Forum*, **31**, 84-89.

[21] Damisih, Jujur, I.N., Sah, J., Agustanhakri and Prajitno, D.H. (2018) Characteristics Microstructure and Microhardness of Cast Ti-6Al-4V ELI for Biomedical Application Submitted to Solution Treatment. *AIP Conference Proceedings*, **1964**, Article ID: 020037. https://doi.org/10.1063/1.5038319